JOURNAL OF APPLIED ELECTROCHEMISTRY 22 (1992) 277–284

Effects of gas bubbles on the current and potential profiles within porous flow-through electrodes

B. E. EL-ANADOULI, B. G. ATEYA

Chemistry Department, Faculty of Science, Cairo University, Cairo, Egypt

Received 2 January 1991; revised 17 June 1991

This paper presents a mathematical model to calculate the distributions of current $i(x)$, potential $E(x)$, gas void fraction $\varepsilon(x)$ and pore electrolyte resistivity $\rho(x)$ within porous flow-through electrodes producing hydrogen. It takes into consideration the following effects: (i) the kinetics of the interfacial charge transfer step, (ii) the effect of the non-uniformly generated gas bubbles on the resistivity of the gas-electrolyte dispersion within the pores of the electrode $\rho(x)$ and (iii) the convective transport of the electrolyte through the pores. These effects appear in the form of three dimensional groups i.e. $K = i_0 \alpha L$ where i_0 is the exchange current density, α is the specific surface area of the electrode and L its thickness. $\phi = \rho^0 L$ where ρ^0 is the pore electrolyte resistivity and $\tau = \sigma/\lambda Q$ where σ is a constant, λ = tortuosity/porosity of the porous electrode and Q is the superficial electrolyte volume flow rate within it. Two more dimensionless groups appear: i.e. the parameter of the ohmic effect $\Delta = K\phi/b$ and the kinetic-transport parameter $I = K\tau$. The model equations were solved for $i(x)$, $E(x)$, $\varepsilon(x)$ and $\rho(x)$ for various values of the above groups.

Nomenclature

α	specific surface area of the bed, area per unit volume (cm^{-1})
b	RT/F in volts, where R is the gas constant, T is the absolute temperature (K)
B	$= [1 - (I^2 Z/4\beta\Delta)]$, Equation 9a
C	$= \sqrt{(1 - B^2)}$, Equation 9b
$E(L)$	potential at the exit face (V)
$E(0)$	potential at the entry face (V)
$E(x)$	potential at distance x within the electrode (V)
E_{rev}	reversible potential of the electrochemical reaction (V)
F	Faraday's constant, 96 500 C eq^{-1}
i_0	exchange current density of the electrode reaction (A cm^{-2} of true surface area)
$i(L)$	current density at the exit face (A cm^{-2} of geometrical cross-sectional area of the packed bed)
I	$K\tau = i_0 \alpha L\ (\sigma/\lambda Q)$ (dimensionless group), Equation 7d
K	$= i_0 \alpha L$, effective exchange current density of the packed bed (A cm^{-2}) Equation 7a
L	bed thickness (cm)
q	tortuosity factor (dimensionless)
Q	superficial electrolyte volume flow rate ($cm^3 s^{-1}$)
x	= position in the electrode (cm)
Z	= exp $[\beta\eta(0)]$, Equation 7f
β	transfer coefficient, $\beta = 0.5$
Δ	$= K\phi/b = (i_0 \alpha L \rho^0 L)/b$ (dimensionless group) Equation 7e
$\varepsilon(x)$	gas void fraction at x (dimensionless)
ϕ	$= \rho^0 L$, effective resistivity of the bubble-free pore electrolyte for the entire thickness of the electrode ($\Omega\,cm^2$)
$\eta(0)$	polarization at the entry face (V)
$\eta(L)$	polarization at the exit face (V)
λ	$= q/\theta$, labyrinth factor
σ	constant ($cm^3\,C^{-1}$), Equation 3a
τ	$= \sigma/\lambda Q\ (A^{-1})$ conversion factor, Equation 3b
θ	porosity of the bed
$\rho(x)$	effective resistivity of the gas-electrolyte dispersion within the pores ($\Omega\,cm$)
ρ^0	effective resistivity of the bubble-free pore electrolyte ($\Omega\,cm$).

1. Introduction

Porous flow-through electrodes have been the subject of intensive research during the last three decades. Their theories of operation and scope of application have been reviewed elsewhere [1–5]. They are characterized by large specific surface areas. When operated in flow-through mode, the rates of mass transfer are enhanced. For these reasons, they have been recommended for use in charging and discharging of redox batteries for load-levelling applications [6, 7], removal of heavy metal ions from waste water streams [8], destruction of cyanide wastes from electroplating baths [9], electrosynthesis [10] and water electrolysis [11]. In many of these applications, there exists a gas-electrolyte dispersion within the pores of the electrode. The gas may be involved in a main reaction or in a parasitic side reaction. Frequently, the gas is non-uniformly generated throughout the pore electrolyte due to the non-uniform distribution of the

0021-891X/92

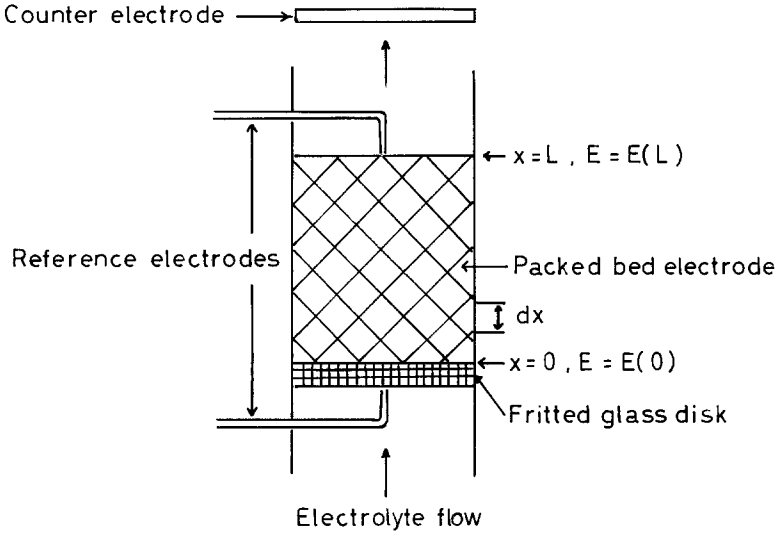

Fig. 1. Schematic illustration of the cell and the experimental arrangements.

reaction. The presence of this gas has a strong influence on the local values of the effective resistivity of the pore electrolyte and hence on the current and potential distributions within the electrode. These effects have been well documented for planar electrodes [12, 13]. The existing theories on the operation of this electrode system are concerned only with electrochemical reactions involving no gaseous reactants or products.

The purpose of this paper is to analyse the effects of gas bubbles on the pore electrolyte resistivity and on the current and potential distributions within the porous electrode. This task is achieved within the framework of a mathematical model which is applied to the case of the hydrogen evolution reaction.

2. Model and assumptions

Figure 1 illustrates the system under consideration. The electrolyte flows upwards while the current flows downwards. The electrolyte is assumed to sweep the bubbles upwards. This is facilitated by the gas lift.

As the electrolyte enters the porous electrode at $x = 0$, it undergoes reaction at a low rate, by virtue of the low potential at $x = 0$. The reaction generates bubbles (at a correspondingly low rate) which disperse in the pore electrolyte and increase its resistivity. A local value of gas void fraction $\varepsilon(x)$ is defined as the fraction of pore space filled by the gas. It is directly proportional to the current density at this distance $i(x)$ (*c.f.* Equation 3). The flow of current through this gas-electrolyte dispersion generates an ohmic potential drop in the pore electrolyte. This results in an increase in potential at larger distances from $x = 0$. As the potential increases, more current is generated, more bubbles are dispersed in the pore electrolyte producing further increase in its resistivity and a greater potential gradient. Consequently the current density $i(x)$, gas void fraction $\varepsilon(x)$, pore electrolyte resistivity $\rho(x)$ and potential $E(x)$ increase non-linearly with distance within the porous electrode. Furthermore, the potential at the entry face $E(0)$ and at the exit face $E(L)$ and the total current output of the electrode $i(L)$ are all interrelated by the governing equations of the model, such that only one of them is an independent variable while the other two are dependent variables.

In developing the model the following assumptions are made. (i) The electrode is a highly interlinked porous medium of high electronic conductivity and small uniform pore size. (ii) Diffuse double layer and ionic migration effects are ignored. (iii) The charge transfer reaction at the electrode-electrolyte interface follows Tafel kinetics, with no concentration polarization. This is quite a suitable assumption for several gas evolution reactions of considerable industrial significance e.g. evolution of hydrogen, oxygen and chlorine. (iv) The gas results from a main reaction. (v) The electrolyte flow is much greater than the gas flow rate. (vi) The resistivity of the electrolyte-bubble dispersion follows the Bruggeman equation (*c.f.* Equation 4) [14]. (vii) Superficial current densities are used i.e. the current densities are calculated on the basis of the cross-sectional area of the packed bed.

Consider a differential space element, dx, of unit cross-sectional area as illustrated in Fig. 1. The current increment $di(x)$ generated in this element is given by

$$\begin{aligned} di(x) &= i_0 \alpha \exp\left[\beta F\{E(x) - E_{rev}\}/RT\right] dx \\ &= i_0 \alpha \exp\left[\beta F \eta(x)/RT\right] dx \end{aligned} \quad (1)$$

where $\eta(x) = E(x) - E_{rev}$ is the local value of polarization. The current is related to the potential (polarization) gradient by Ohm's law i.e.

$$i(x) = [1/\rho(x)]\, d\eta(x)/dx \quad (2)$$

where $\rho(x)$ is the effective resistivity of the pore electrolyte at distance x. The resulting gas creates voids in the flowing electrolyte. The gas void fraction is related to the current by [15]

$$\varepsilon(x) = \frac{\sigma}{\lambda Q} i(x) \quad (3a)$$

$$= \tau\, i(x) \quad (3b)$$

hence $\tau = \sigma/\lambda Q$, where σ is a constant of a chemical nature which equals $0.127\,cm^3\,C^{-1}$ for hydrogen evolution at 25°C and 1 atm, $\lambda = q/\theta$ is the labyrinth

factor, q is the tortuosity, θ is the porosity of the bed, and Q is the superficial electrolyte flow rate. For normal porous solids where $\sqrt{2} < q < 4$ and $0.2 < \theta < 0.7$, λ ranges from 2 to 20. Equation 3 has been derived elsewhere [15] for the conditions of large electrolyte flow rate compared to gas flow rate. The resistivity of the gas-electrolyte dispersion within the pores is given by the Bruggeman equation [14] i.e.

$$\rho(x) = \rho^0[1 - \varepsilon(x)]^{-3/2} \tag{4}$$

The boundary conditions are

$$x = 0, \quad i(x) = 0, \quad \eta(x) = \eta(0) \tag{5a}$$

$$x = L, \quad i(x) = i(L), \quad \eta(x) = \eta(L) \tag{5b}$$

The objective now is to solve this system of equations for the distributions of $i(x)$, $\varepsilon(x)$, $\rho(x)$, and $E(x)$, subject to the above boundary conditions. The effects of the various system parameters on these distributions are evaluated and discussed.

3. Solution of the model equations

The above system of equations was normalized and solved for one step [15] to give

$$d\bar{i}(\bar{x})/d\bar{x} = \exp[\beta\bar{\eta}(\bar{x})] \tag{6a}$$

$$= \frac{2\beta\Delta}{I^2}\left(\frac{2 - I\bar{i}(\bar{x})}{\{1 - I\bar{i}(\bar{x})\}^{1/2}}\right) - \frac{4\beta\Delta}{I^2} + Z \tag{6b}$$

where the variables with overbars denote normalized variables i.e. $\bar{x} = x/L$, $\bar{i}(\bar{x}) = i(x)/i_0\alpha L$, $\bar{\eta}(\bar{x}) = \eta(x)/b = [E(x) - E_{rev}]/b$, $b = RT/F$ in volt and $\bar{\rho}(\bar{x}) = \rho(x)/\rho^0$. Henceforth, the overbars are dropped for algebraic convenience. As a result of normalization, the following dimensional and dimensionless groups appear:

$$K = i_0\alpha L \tag{7a}$$

$$\tau = \sigma/\lambda Q \tag{7b}$$

$$\phi = \rho^0 L \tag{7c}$$

$$I = K\tau = i_0\alpha L\sigma/\lambda Q \tag{7d}$$

$$\Delta = K\phi/b = (i_0\alpha L\rho^0 L)F/RT \tag{7e}$$

$$Z = \exp[\beta\eta(0)] \tag{7f}$$

The dimensionless group $\Delta = K\phi/b$ is an index of the ohmic effect. It is the ohmic potential drop in units of b which results if a current of $i_0\alpha L$ is transported through the pore electrolyte over the entire thickness of the electrode, in the absence of gas bubbles. It relates the ohmic resistance of the pore electrolyte, the electrode thickness, the structural properties of the electrode and the electrocatalytic properties of the system.

The dimensionless groups Δ and I are products of dimensional groups pertaining to the electrocatalytic (kinetic), resistive and transport properties of the system. Thus K is the overall exchange current of the entire porous electrode (per unit geometrical area). The product $\phi = \rho^0 L$ is the pore electrolyte resistance (in the absence of bubbles) for the entire thickness and unit geometrical area of the porous electrode. The transport parameter $\tau = \sigma/\lambda Q$ is essentially a conversion factor which converts current density into gas void fraction through dependence on σ which is of chemical nature, λ which relates to the structural properties of the electrode and Q which is the superficial electrolyte flow rate. An increase in λ and/or Q results in a decrease in the gas void fraction $\varepsilon(x)$ (see Equation 3a).

Equation 6b relates the current and potential in terms of the system parameters i.e. β, Δ, I, etc. It must be further integrated to give the current as a function of distance. The details are given in Appendix 1 and the solution is

$$\frac{2B^2 - 1}{C}\left\{\tan^{-1}\left[\frac{\sqrt{(1 - Ii(x))} - B}{C}\right] - \tan^{-1}\left[\frac{\sqrt{(1 - Ii(L))} - B}{C}\right]\right\} + B\ln\left\{\frac{2 - 2B\sqrt{(1 - Ii(x))} - Ii(x)}{2 - 2B\sqrt{(1 - Ii(L))} - Ii(L)}\right\} + \{\sqrt{(1 - Ii(x))} - \sqrt{(1 - Ii(L))}\} = \frac{\beta\Delta}{I}[1 - x] \tag{8}$$

where

$$B = \left[1 - \frac{I^2 Z}{4\beta\Delta}\right] \tag{9a}$$

and

$$C = \sqrt{(1 - B^2)} \tag{9b}$$

Equation 8 gives the current profile within the electrode, in terms of the system parameters β, Δ, I and Z and the total current $i(L)$. In order to use Equation 8 to calculate current profiles, the value of $i(L)$ corresponding to a certain value of $\eta(0)$ must be known and hence the value of Z. This value of $i(L)$ is not known as yet, since $\eta(0)$ relates to the entry face of the electrode while $i(L)$ relates to the exit face. Note that $\eta(0)$, $i(L)$ and $\eta(L)$ are all related in such a way that only one of them is an independent variable while the other two are dependent on the former. The interdependence of these variables becomes evident upon consideration of the physical picture and the governing equations of the system (see above under model and assumptions). Fortunately, the dependence of $i(L)$ on $\eta(0)$ can be obtained in a closed form, albeit complicated, by applying Equation 8 at the boundary condition, i.e. at $x = 0$, $i(x) = 0$. Thus,

$$\frac{2B^2 - 1}{C}\left\{\tan^{-1}\left[\frac{1 - B}{C}\right] - \tan^{-1}\left[\frac{\sqrt{(1 - Ii(L))} - B}{C}\right]\right\} + B\ln\left\{\frac{2(1 - B)}{2 - 2B\sqrt{(1 - Ii(L))} - Ii(L)}\right\} + \left\{1 - \sqrt{(1 - Ii(L))}\right\} = \beta\Delta/I \tag{10}$$

The last equation relates the total current produced by the electrode, $i(L)$, to the level of polarization at the entry face, $\eta(0)$, through β, Δ, I and Z. Using Equation 10, the value of $i(L)$ which corresponding to a chosen value of $\eta(0)$ can be calculated. Knowing $\eta(0)$ and $i(L)$, Equation 8 can be solved for the current profile. The resulting current/distance data are then applied in Equations 3a, 4 and 6a to obtain profiles of void fraction $\varepsilon(x)$, pore electrolyte resistivity $\rho(x)$ and potential $\eta(x)$, respectively.

4. Results and discussion

Much like the case in porous catalysts, the behaviour of a porous electrode may be controlled by the rates of the electrochemical reaction at the electrode/electrolyte interface and/or the diffusion process. In addition, the behaviour of the electrode may also be controlled by the ohmic potential drop through the pore electrolyte. The combined effects of the above controlling steps result in non-uniform distributions of current and potential within the electrode. The literature has references to several analytical [16] and numerical solutions [17–19] of current and potential distributions within porous electrodes for simple redox reactions in the absence of gas bubbles.

In the present system, there is no diffusion control [11, 20], but the system is complicated by the effects of the non-uniformly generated gas bubbles. The profiles of $i(x)$, $\eta(x)$, $\varepsilon(x)$, and $\rho(x)$, as well as the overall behaviour of the electrode depend on the dimensionless groups Δ, I and Z. The index of ohmic effect $\Delta = i_0 \alpha L \rho^0 L/b$ is a product of a kinetic ($i_0 \alpha L$) and an ohmic ($\rho^0 L$) parameters, while I is a product of the kinetic ($i_0 \alpha L$) and transport ($\sigma/\lambda Q$) parameters. Furthermore, Z depends on the transfer coefficient β and the level of polarization at the entry face of the electrode, $\eta(0)$. Through the following discussion we take an electrode with known values of i_0, α and L and evaluate the effects of the operational variables ρ^0, τ and $\eta(0)$ on the profiles of potential, current, gas void fraction and resistivity.

4.1. *Potential distribution*

The level of polarization at the entry face $\eta(0)$ has a significant effect on the potential profile, as shown in Fig. 2. The potential profile is much sharper and the bubble effect becomes more pronounced at higher, than at lower, $\eta(0)$ values. However the bubbles have only a small effect on the polarization profile.

The effect of the transport parameter τ on the potential profile is shown in Fig. 3 for $\rho^0 = 104.6\,\Omega$cm and $\eta(0) = 13.2$. As τ decreases i.e. as the electrolyte flow rate becomes much larger than the gas flow rate (see Equation 3a), the potential profile becomes less sharp i.e. the system is under a smaller degree of ohmic control. This is because a smaller τ corresponds to a smaller value of $\varepsilon(x)$, and hence a smaller value of effective resistivity of the gas-electrolyte dispersion within the pores. The effect of ρ^0 on the polarization

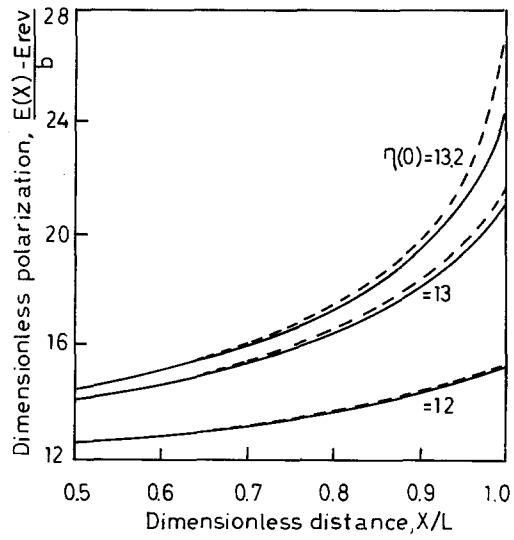

Fig. 2. Effect of gas bubbles on the polarization profiles within the packed bed electrode at various values of $\eta(0)$ and $\rho^0 = 104.6\,\Omega$cm. (——) No bubbles, (– – –) bubbles.

profile was also calculated. It was found that as ρ^0 increases, the profile becomes sharper. The bubble effect was found to be comparable to that in Fig. 2. The results show that the potential drop within the pore electrolyte i.e. $\Delta E = E(L) - E(0)$ increases as ρ^0, $\eta(0)$, and/or τ increase and hence also the potential at the exit face of the electrode $E(L)$. Under a certain set of conditions, ΔE is greater in the presence than in the absence of gas bubbles.

4.2. *Current distribution*

Figures 4 and 5 illustrate the effects of gas bubbles, polarization level $\eta(0)$, and bubble-free pore electrolyte resistivity ρ^0 on the current distribution. The values of $\eta(0)$ and ρ^0 determine whether the current distribution is more or less uniform and whether the bubble effect is significant or not. At larger values of $\eta(0)$ and ρ^0, the presence of gas bubbles has a pronounced effect on

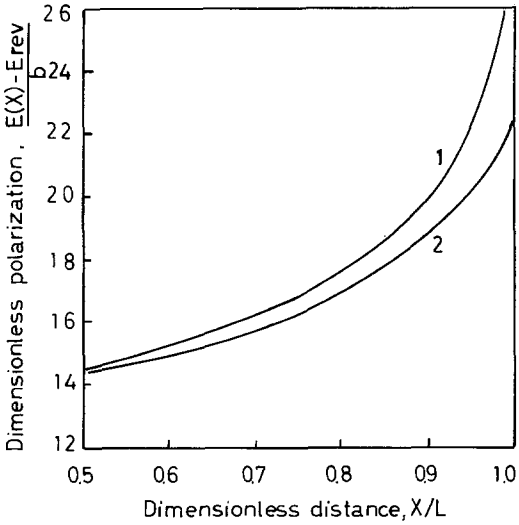

Fig. 3. Effect of the transport parameter τ on the polarization profile at $\eta(0) = 13.2$ and $\rho^0 = 104.6\,\Omega$cm. (1) $\tau = 1.27$ and (2) $\tau = 0.127$.

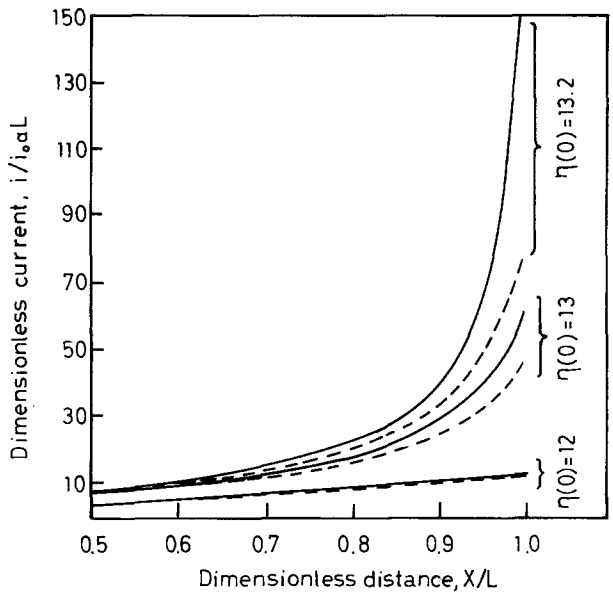

Fig. 4. Effect of gas bubbles on the current distribution within packed bed electrode at various values of $\eta(0)$, $\rho^0 = 104.6\,\Omega$cm. (——) No bubbles, (- - -) bubbles.

the magnitude of current and on its distribution. On the other hand, gas bubbles have only negligible effects at smaller values of $\eta(0)$ and ρ^0. Alternatively, at larger values of $\eta(0)$ and ρ^0, the current distribution is much more non-uniform than at smaller values. Thus at $\eta(0) = 12$ the current is rather uniformly distributed within the entire thickness of the electrode (as revealed by the almost linear relation of $i(x)$ against x), and the presence of gas bubbles has only a negligible influence on the current profile. On the other hand, at $\eta(0) = 13.2$, the current profile is rather non-uniform i.e. the major part of the reaction occurs in a skin layer near the exit face of the electrode, of about 10–15% of the electrode thickness i.e. $(0.85 < x < 1.0)$. Furthermore, in this region, the bubbles have a large effect on the magnitude of the current, their effect depends on

Table 1. Effect of transport parameter τ on the relation between $\eta(0)$, $\eta(L)$, and $i(L)$ at $\rho^0 = 104.6\,\Omega$cm

$\eta(0)$	$\eta(L)$		$i(L)$	
	$\tau = 0.127$	$\tau = 1.27$	$\tau = 0.127$	$\tau = 1.27$
5.00	5.032	5.076	0.215	0.215
10.00	11.002	11.009	3.074	3.027
12.00	15.150	15.376	12.212	12.147
13.00	20.137	21.669	45.970	45.931
13.05	–	22.200	–	50.470
13.10	21.128	23.419	58.691	58.454
13.20	22.174	27.160	75.619	75.477

the level of polarization at the entry face. Thus at $\eta(0)$ of 13.2 and $\rho^0 = 104.6\,\Omega$cm, the current $i(L)$ in presence of bubbles is only one-half of its value in their absence and the $\eta(L)$ values are 27.16 and 24.61, respectively, while at $\eta(0) = 12$ there is no significant effect of bubbles neither on the current profile nor on the current output.

To illustrate the effect of the transport parameter, τ, on the current distribution within the electrode, its effect on the polarization at the exit face, $\eta(L)$ must be known. Table 1 shows the effect of τ on the relation between $\eta(0)$, $\eta(L)$, and $i(L)$. The table reveals that for a certain value of $\eta(0)$ an increase in τ results in an increase in $\eta(L)$ which influences $i(L)$ and, hence, the current distribution $i(x)$. Consequently, the effect of τ on the current distribution must be compared at comparable $\eta(L)$ values. This is the reason for including in Table 1, the results at $\eta(0) = 13.05$ for $\tau = 1.27$, which are to be compared with those at 13.2 for $\tau = 0.127$, since $\eta(L)$ is about equal in both cases. The comparison is shown in Fig. 6. Clearly, the figure shows that the increase in τ results in less non-uniform distribution of the current. This is in accord with the physical reasoning since the decrease in τ corresponds to a decrease in the gas void fraction $\varepsilon(x)$, which

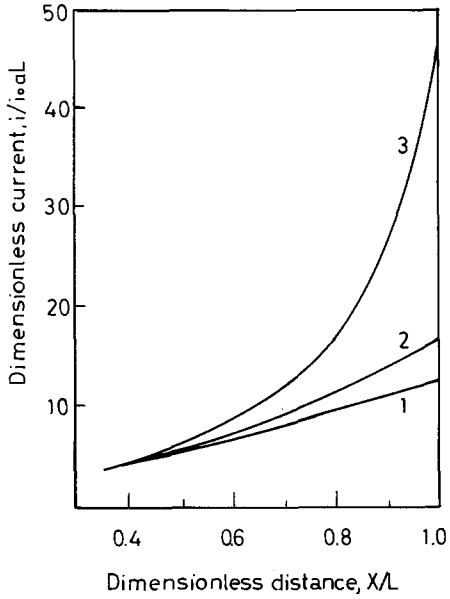

Fig. 5. Effect of the pore electrolyte resistivity on the current distribution within the packed bed electrode at $\eta(0) = 13.0$. ρ^0/Ωcm: (1) 5.25, (2) 52.3 and (3) 104.6.

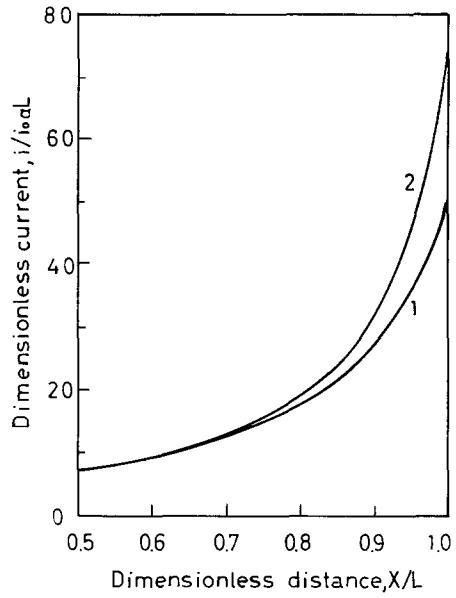

Fig. 6. Effect of the transport parameter τ on the current distribution within the packed bed electrode at $\eta(0) = 13.2$ and $\rho^0 = 104.6\,\Omega$cm. (1) $\tau = 1.27$ and (2) $\tau = 0.127$.

Table 2. Effects of ρ^0 and $\eta(L)$ on the half-current distance, x (0.5)

ρ^0 Ω cm	$x(0.5)$					
	$\eta(0)$	5	10	12	13	13.2
5.25		0.500	0.500	0.500	0.500	0.500
52.20		0.502	0.526	0.579	0.645	0.665
104.60		0.504	0.560	0.700	0.880	0.919

results in a decrease in the effective resistivity of the gas-electrolyte dispersion filling the pore. We have already shown above (Fig. 5) that as the resistivity of the pore electrolyte decreases, the reaction distribution becomes less non-uniform.

Figures 4 to 6 further show that at higher values of $\eta(0)$, ρ^0 and/or τ the interior of the electrode ($x < 0.6$) is not well utilized, while the intermediate region ($0.6 < x < 0.9$) is only moderately utilized. The optimum utilization is in a skin layer ($0.9 < x < 1$) near the exit face of the electrode. This is a conclusion which may prove useful for design purposes. It has important practical implications i.e. a small amount of a good electrocatalytic material might be loaded onto this skin layer to reduce the magnitude of the activation polarization and hence power consumption.

The above conclusions are presented in a more quantitative form in Table 2, which lists the parameters influencing the non-uniformity of current distribution along with their effects on the extent of non-uniformity. For reasons of simplicity and brevity, only one criterion is selected to gauge the non-uniformity of the current distribution. This is the half-current distance, $x(0.5)$, which is the distance at which the local value of current $i(0.5)$ is one-half of the total current output, $i(L)$. For uniform current distribution $x(0.5)$ must be 0.5. The extent of deviation of $x(0.5)$ from 0.5 is taken as a measure of the extent of non-uniformity. The table clearly shows that increases in ρ^0 and/or $\eta(0)$ lead to progressively non-uniform distributions of current and potential.

4.3. *Distribution of $\varepsilon(x)$ and $\rho(x)$*

Figures 7 to 9 illustrate the profiles of gas void fraction within the electrode $\varepsilon(x)$ at various values of $\eta(0)$, ρ^0 and τ. The distribution of $\varepsilon(x)$ is quite non-uniform at higher, than at lower, values of $\eta(0)$, ρ^0 and τ. For instance, at $\rho^0 = 104.6\,\Omega$cm, the gas void fraction drops to about half of its value through only one tenth of the electrode thickness (i.e. $0.9 < x < 1.0$), while the comparable decrease at $\rho^0 = 5.25\,\Omega$cm occurs over practically half the electrode thickness.

As mentioned earlier, the pore electrolyte resistivity is related to the gas void fraction by Equation 4. By virtue of this equation, a linear change in $\varepsilon(x)$ leads to an exponential change in $\rho(x)$. This is clear from Fig. 10 which illustrates the profiles of pore electrolyte resistivity for the conditions of Fig. 9. Note the sharp increase in $\rho(x)/\rho^0$ at $x > 0.9$ for $\tau = 1.27$. Some numerical calculations are useful at this point. Consider the case where $\rho^0 = 104.6\,\Omega$cm and $\eta(0) = 13.2$. Between $x = 0.9$ and $x = 1.0$, $\varepsilon(x)$ changes from 0.48 to 0.96 and consequently the corresponding resistivities jump from $2.7\,\rho^0$ to $125\,\rho^0$. This sharp increase in $\rho(x)$ must result in a corresponding decrease in $i(x)$, since as we have seen before, $E(x)$ changes only slightly by the presence of bubbles. This calculation is only meant to illustrate the effect of bubbles on the pore electrolyte resistivity at high values of gas void fraction. The present model was developed for the case of small values of $\varepsilon(x)$. Hence the calculations are more accurate at lower than at higher values of $\varepsilon(x)$.

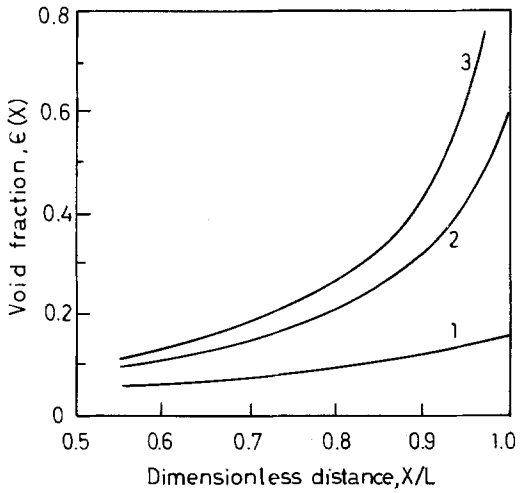

Fig. 7. Effect of $\eta(0)$ on the profile of gas void fraction, $\rho^0 = 104.6\,\Omega$cm. $\eta(0)$: (1) 12.0, (2) 13.0 and (3) 13.2.

5. Summary and conclusions

1. At smaller values of $\eta(0)$ and/or ρ^0, the presence of gas bubbles has only a negligible influence on the distributions of current and potential and hence on the behaviour of the electrode.

2. At higher values of $\eta(0)$ and/or ρ^0 the presence of gas bubbles has strong effects on the distributions of

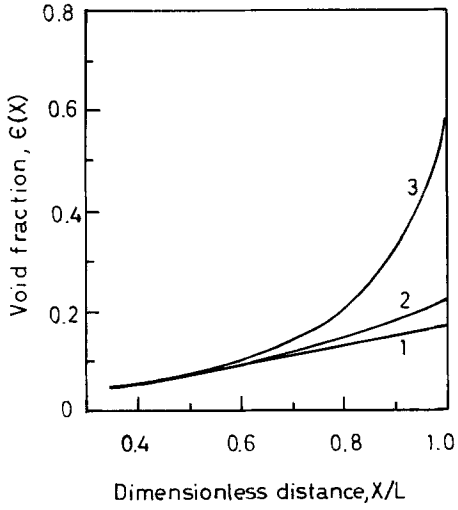

Fig. 8. Effect of the pore electrolyte resistivity on the profile of gas void fraction within the packed bed electrode, at $\eta(0) = 13.0$. ρ^0/Ωcm: (1) 5.25, (2) 52.3 and (3) 104.6.

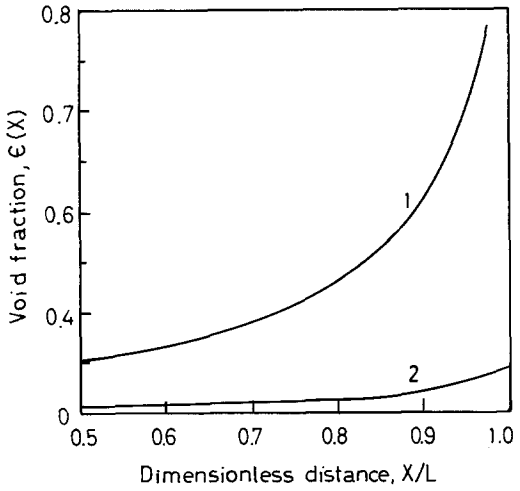

Fig. 9. Effect of the transport parameter τ on the profile of gas void fraction at $\eta(0) = 13.2$ and $\rho^0 = 104.6\,\Omega$cm. (1) $\tau = 1.27$ and (2) $\tau = 0.127$.

current, potential, gas void fraction and pore electrolyte resistivity. The effect on the potential distribution is less pronounced.

3. As $\eta(0)$, ρ^0 and/or τ increase the profiles of $i(x)$, $\eta(x)$, $\varepsilon(x)$ and $\rho(x)$ become more non-uniform.

4. The effects of variations in τ on the profiles are much less pronounced than those in $\eta(0)$ or ρ^0.

5. At higher values of $\eta(0)$, ρ^0 and/or τ the interior of the electrode ($0 < x < 0.6$) is not well utilized, while the intermediate region ($0.6 < x < 0.9$) is only moderately utilized.

6. The optimum utilization of the electrode is in a skin layer ($0.9 < x < 1.0$) near the exit surface of the electrode. This conclusion may prove useful in design considerations. It suggests that a small amount of a good electrocatalytic material might be loaded onto this skin layer to reduce the magnitude of activation polarization and hence power consumption.

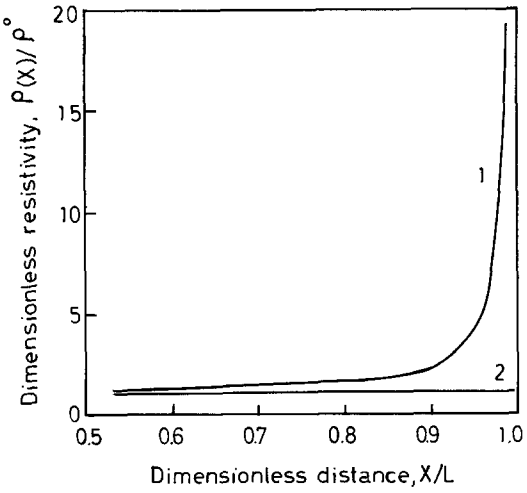

Fig. 10. Effect of the transport parameter τ on the profile of pore electrolyte resistivity within the packed bed electrode at $\eta(0) = 13.2$ and $\rho^0 = 104.6\,\Omega$cm. (1) $\tau = 1.27$ and (2) $\tau = 0.127$.

References

[1] R. de Levie, in 'Advances in Electrochemistry and Electrochemical Engineering' Vol 6 (edited by P. Delahy) Interscience, New York (1967).
[2] J. Newman and W. Tiedman, 'Advances in Electrochemistry and Electrochemical Engineering', Vol. 11 (edited by H. Gerischer and C. W. Tobias) J. Wiley & Sons, New York (1976) p. 352.
[3] R. E. Sioda and K. B. Keating, 'Electroanalytical Chemistry', Vol. 12 (edited by A. J. Bard) Marcel Dekker, New York (1982).
[4] F. Goodridge and A. R. Wright, Porous Flow-Through and Fluidized Bed Electrodes, in 'Comprehensive Treatise of Electrochemistry' Vol. 6, Electrochemical Processing, (edited by J. O'M. Bockris, B. E. Conway, E. Yeager and R. E. White), Plenum Press, New York (1984) chap. 6.
[5] N. A. Hampson and A. J. S. McNeil, 'The Electrochemistry of Porous Electrodes, Flow-Through and Three Phases Electrodes'. 'Electrochemistry', Vol. 9, The Royal Society of Chemistry, London (1984) p. 1–65.
[6] M. Warshy and L. O. Wright, *J. Electrochem. Soc.* **124** (1977) 173.
[7] K. Kinoshita and S. C. Leach, *ibid.* **129** (1982) 1993.
[8] D. N. Bennion and J. Newman, *J. Appl. Electrochem.* **2** (1972) 113.
[9] D. T. Chin and B. Eckert, *Plat. Surf. Finish.* **10** (1976) 38.
[10] C. Oloman, *J. Electrochem. Soc.* **126** (1979) 1885.
[11] B. G. Ateya and E. S. Arafat, *ibid.* **130** (1983) 380.
[12] P. J. Sides in 'Modern Aspects of Electrochemistry' No. 18 (edited by R. E. White, J. O'M. Bockris and B. E. Conway), Plenum, New York (1986).
[13] H. Vogt, in 'Comprehensive Treatise of Electrochemistry' Vol. 6, Plenum Press, New York (1983).
[14] C. W. Tobias and R. E. Meredith in 'Advances in Electrochemistry and Electrochemical Engineering', Vol. 2, Interscience, New York (1962).
[15] B. G. Ateya and B. E. El-Anadouli, *J. Electrochem. Soc.* **138** (1991) 1331.
[16] L. G. Austin and E. G. Gagnon, *AIChE J.* **17** (1971) 1057.
[17] J. Newman and C. W. Tobias, *J. Electrochem. Soc.* **109** (1962) 1183.
[18] J. A. Trainham and J. Newman, *ibid.* **124** (1977) 1528.
[19] R. Alkire and B. Gracon, *ibid.* **122** (1975) 1594.
[20] B. E. El-Anadouli, M. M. Khader, M. M. Saleh and B. G. Ateya, *J. Appl. Electrochem.* **21** (1991) 166.

Appendix 1

This appendix summarizes the derivation of Equation 8 in the preceding text.

$$\frac{di(x)}{dx} = \frac{2\beta\Delta}{I^2}\left[\frac{2 - Ii(x)}{\sqrt{(1 - Ii(x))}}\right] - \frac{4\beta\Delta}{I^2} + Z \qquad \text{(A1)}$$

Let

$$T^2 = 1 - Ii(x) \qquad \text{(A2)}$$

Then,

$$2T\,dt = -I\,di \qquad \text{(A3)}$$

$$\frac{di(x)}{dx} = \frac{-2T\,dT}{I\,dx}$$

$$= \frac{2\beta\Delta}{I^2}\left[1 + T^2 + \left(\frac{ZI^2}{2\beta\Delta} - 2\right)T\right]dx \qquad \text{(A4)}$$

Rearranging

$$\int \frac{T^2\,dT}{1 - 2BT + T^2} = \frac{-\beta\Delta}{I}\int dx \qquad \text{(A5)}$$

Where

$$\frac{ZI^2}{2\beta\Delta} - 2 = -2B \qquad \text{(A6)}$$

Integrating Equation A5 using Equation A2 gives

$$\sqrt{(1 - Ii(x))} + B \ln [1 - B\sqrt{(1 - Ii(x))} + \{1 - Ii(x)\}] + (2B^2 - 1) \times \left[\frac{1}{C} \tan^{-1} \frac{\sqrt{(1 - Ii(x))} - B}{C}\right] = -\frac{\beta\Delta}{I} x + \text{constant} \quad \text{(A7)}$$

Where

$$C = \sqrt{(1 - B^2)} \quad \text{(A8)}$$

Using the boundary conditions

$$\text{at } x = 1; \quad i(x) = i(L)$$

Equation A7 becomes

$$\frac{2B^2 - 1}{C} \left\{\tan^{-1}\left[\frac{\sqrt{(1 - Ii(x))} - B}{C}\right] - \tan^{-1}\left[\frac{\sqrt{(1 - Ii(L))} - B}{C}\right]\right\} + B \ln \left\{\frac{2 - 2B\sqrt{(1 - Ii(x))} - Ii(x)}{2 - 2B\sqrt{(1 - Ii(L))} - Ii(L)}\right\} + \{\sqrt{(1 - Ii(x))} - \sqrt{(1 - Ii(L))}\} = \frac{\beta\Delta}{I}(1 - x) \quad \text{(A9)}$$